



HAL
open science

Potential of enriched phototrophic purple bacteria for H₂ bioconversion into single cell protein

María del Rosario Rodero, Jose Antonio Magdalena, Jean-Philippe Steyer, Renaud Escudié, Gabriel Capson-Tojo

► **To cite this version:**

María del Rosario Rodero, Jose Antonio Magdalena, Jean-Philippe Steyer, Renaud Escudié, Gabriel Capson-Tojo. Potential of enriched phototrophic purple bacteria for H₂ bioconversion into single cell protein. *Science of the Total Environment*, 2024, 908, pp.168471. 10.1016/j.scitotenv.2023.168471 . hal-04284364

HAL Id: hal-04284364

<https://hal.inrae.fr/hal-04284364>

Submitted on 14 Nov 2023

HAL is a multi-disciplinary open access archive for the deposit and dissemination of scientific research documents, whether they are published or not. The documents may come from teaching and research institutions in France or abroad, or from public or private research centers.

L'archive ouverte pluridisciplinaire **HAL**, est destinée au dépôt et à la diffusion de documents scientifiques de niveau recherche, publiés ou non, émanant des établissements d'enseignement et de recherche français ou étrangers, des laboratoires publics ou privés.

Journal Pre-proof

Potential of enriched phototrophic purple bacteria for H₂ bioconversion into single cell protein

María del Rosario Rodero, Jose Antonio Magdalena, Jean-Philippe Steyer, Renaud Escudié, Gabriel Capson-Tojo



PII: S0048-9697(23)07099-7

DOI: <https://doi.org/10.1016/j.scitotenv.2023.168471>

Reference: STOTEN 168471

To appear in: *Science of the Total Environment*

Received date: 19 July 2023

Revised date: 20 October 2023

Accepted date: 8 November 2023

Please cite this article as: M. del Rosario Rodero, J.A. Magdalena, J.-P. Steyer, et al., Potential of enriched phototrophic purple bacteria for H₂ bioconversion into single cell protein, *Science of the Total Environment* (2023), <https://doi.org/10.1016/j.scitotenv.2023.168471>

This is a PDF file of an article that has undergone enhancements after acceptance, such as the addition of a cover page and metadata, and formatting for readability, but it is not yet the definitive version of record. This version will undergo additional copyediting, typesetting and review before it is published in its final form, but we are providing this version to give early visibility of the article. Please note that, during the production process, errors may be discovered which could affect the content, and all legal disclaimers that apply to the journal pertain.

© 2023 Published by Elsevier B.V.

Potential of enriched phototrophic purple bacteria for H₂ bioconversion into single cell protein

María del Rosario Rodero^{a,b,c*}, Jose Antonio Magdalena^{a,d}, Jean-Philippe Steyer^a, Renaud Escudie^a, Gabriel Capson-Tojo^a

^a INRAE, Univ Montpellier, LBE, 102 Avenue des Etangs, 11100 Narbonne, France

^b Institute of Sustainable Processes, University of Valladolid, Dr. Mergelina, s/n, 47011 Valladolid, Spain

^c Department of Chemical Engineering and Environmental Technology, School of Industrial Engineering, University of Valladolid, Dr. Mergelina s/n, 47011 Valladolid, Spain

^d Vicerrectorado de Investigación y Transferencia de la Universidad Complutense de Madrid, 28040 Madrid, Spain

*corresponding author: maria-del-rosario.rodero-roya@inrae.fr / mariarosario.rodero@uva.es

Abstract

Single cell protein (SCP) has emerged as an alternative protein source, potentially based on the recovery of carbon and nutrients from waste-derived resources as part of the circular economy. From those resources, gaseous substrates have the advantage of an easy sterilization, allowing the production of pathogen-free SCP. Sterile gaseous substrates allow producing pathogen-free SCP. This study evaluated the use of an enriched phototrophic purple bacteria (PPB) consortium for SCP production using H₂ and CO₂ as electron and C sources. The influence of pH (6.0-8.5), temperature (15-50 °C) and light intensity (0-50 W·m⁻²) on the growth kinetics and biomass yields was investigated using batch tests. Optimal conditions were found at pH 7, 25 °C and light intensities over 30 W·m⁻². High biomass and protein yields were achieved (~ 1 g COD_{biomass}·g COD_{H₂consumed}⁻¹ and 3.9-4.4 g protein·g H₂⁻¹)

regardless of the environmental conditions, being amongst the highest values reported from gaseous streams. These high yields were obtained thanks to the use of light as a sole energy source by the PPB consortium, allowing a total utilization of H₂ for growth. Hydrogen uptake rates varied considerably, with values up to 61±5 mg COD·d⁻¹ for the overall H₂ consumption rates and 2.00±0.14 g COD·g COD⁻¹·d⁻¹ for the maximum specific uptake rates under optimal growth conditions. The latter value was estimated using a mechanistic model able to represent PPB growth on H₂. The biomass exhibited high protein contents (>50% w/w) and adequate amino acid profiles, showing its suitability as SCP for feed. PPB were the dominant bacteria during the experiments (relative abundance over 80% in most tests), with a stable population dominated by *Rhodobacter* sp. and *Rhodopseudomonas* sp. This study demonstrates the potential of enriched PPB cultures for H₂ bioconversion into SCP.

Keywords: anoxygenic photosynthesis; autotrophy; hydrogen; purple non-sulphur bacteria; mechanistic modelling

1. Introduction

Sustainable food and feed production is nowadays a serious global concern due to population growth, climate change and limited natural resources. The global population has increased from 2.5 to 8.0 billion people since 1950 and it is expected to reach 9.7 billion by 2050 (United Nations Department of Economic and Social Affairs, 2022). Current human diets rely on conventional agriculture, farming and fishing. These activities have associated problems such as high greenhouse gas emissions, nitrogen losses, pesticides and antibiotics pollution, and land, nutrients and water depletion (Ciani et al., 2019). Therefore, there is an urgent need to develop new sustainable food and feed alternatives, especially for products used as a protein source. Proteins play a key role in human and animal diet as a source of nitrogen and

essential amino acids (Ritala et al., 2017). The demand for protein has increased 5-fold in the last 50 years, reaching a consumption of 250 million tonnes in 2020 due to a change in consumption habits and higher living standards worldwide (Bertasini et al., 2022).

The use of microorganisms as a protein-rich feedstock, the so-called single cell protein (SCP), is a promising alternative to plant or animal-based proteins, since microorganisms can use resources such as nutrients (e.g. nitrogen and phosphorous) or water more efficiently (Puyol et al., 2017b). The production of SCP avoids some of the environmental drawbacks of plant- or animal-based proteins, through reduced land requirements, lower nitrogen losses, lower emissions of greenhouse gases and smaller water footprints (Alloul et al., 2022). Some SCP products are commercially available for animal feed and human food supplements, mainly from yeast, microalgae, fungi and bacteria (e.g. methylophs, acetotrophs and hydrogen oxidizing bacteria (HOB)) (Sharif et al., 2021). Despite the aforementioned advantages, current SCP is mostly produced from costly agricultural feedstocks or unsustainable raw materials such as sucrose, starch, n-alkanes, fossil-derived methanol or natural gas (Nasseri et al., 2011). This reduces the environmental benefits of using SCP as alternative protein source. A potential alternative to the unsustainable feedstocks mentioned above is the utilisation of waste-derived resources for the production of SCP. This approach, generally referred to as biological resource recovery, has been widely researched in the last years, aiming at favouring the implementation of a more circular economy. Amongst all the different options that can be used as substrates for resource recovery, gaseous substrates (e.g., H₂, CO₂ and/or CH₄) have a huge advantage over other alternatives (e.g., soluble compounds in wastewaters): they can be easily sterilized, simply by filtering the gaseous input. This is crucial for ensuring the safety of the generated product, which is particularly important for SCP within the food industry. Furthermore, the influent composition is relatively easy to measure, manipulate and maintain by simply controlling the gas flowrate, facilitating the generation of a consistent product.

Coupled with well-established gas-producing waste treatment technologies such as anaerobic digestion or dark fermentation, the valorisation of the generated gases (CH_4 , CO_2 and H_2) by their transformation into SCP has the potential to produce a high value product, while providing a more sustainable alternative to traditional protein production. Ideally, the nutrients (*e.g.*, N or P) for biomass growth should be safely recovered (*e.g.* via electrochemical processes or membranes) from waste effluents (*e.g.*, from wastewater or anaerobic digestate) (Khoshnevisan et al., 2019; Matassa et al., 2015).

The feasibility of using H_2 and CO_2 as raw materials for the production of SCP by HOB has been demonstrated (Hu et al., 2022). Despite the high quality of the biomass obtained, the low biomass yields ($0.07\text{-}0.20 \text{ g COD}\cdot\text{g COD}_{\text{H}_2}^{-1}$; COD being chemical oxygen demand), which result in the need of high amounts of H_2 for biomass production, is one of the main bottlenecks of this technology (Ehsani et al., 2019; Hu et al., 2020). The use of purple phototrophic bacteria (PPB) grown on pathogen-free gases is another interesting option for safe SCP production. Compared to HCB, PPB can potentially offer higher biomass yields (*i.e.*, 1 vs. 0.2 $\text{g COD}\cdot\text{g COD}_{\text{removed}}^{-1}$), while having also a high content on amino acids, pigments and vitamins (Hülsemann et al., 2018; Sasaki et al., 1998). These high biomass yields represent the most relevant advantage of PPB compared with non-phototrophic microorganisms, since the latter consume substrate for internal energy production (*e.g.* ATP). PPB use light for this. Therefore, lower amount of substrate is needed to produce the same amount of biomass. PPB exhibit a highly versatile metabolism, capable of performing anoxygenic photosynthesis, using solar light as energy source, and a wide range of electron/carbon donors such as organic compounds (photoheterotrophic growth), or $\text{H}_2/\text{H}_2\text{S}$ with CO_2 as carbon source (chemolithoautotrophic and photoautotrophic growth) (Capson-Tojo et al., 2020). The photoheterotrophic capabilities of PPB have been explored considerably in the recent years for resource recovery from wastewaters (Alloul et al., 2019;

Hülßen et al., 2022c, 2022b). However, the use of H₂ for PPB growth has received less attention (Madigan and Gest, 1979; Rey et al., 2006; Spanoghe et al., 2022, 2021).

The uptake by PPB of H₂ from processes such as dark fermentation or gasification (in the form of syngas), or from water electrolysis using surplus of electricity from renewable sources, could be a promising option for the sustainable and pathogen-free production of SCP usable as feed/food. In this context, this process could be integrated as a part of a future hydrogen biorefinery. CO₂ from off-gases could be used as carbon source. The proof of concept of SCP production from H₂ using PPB pure cultures and autotrophic isolates has been recently conducted (Spanoghe et al., 2022, 2021). In this regard, the use of a mixed culture for the production of animal feed would lead to cost reduction due to non-sterile conditions. Indeed, the suitability of a heterotrophic PPB mixed culture as a partial substitute of fishmeal has been previously demonstrated (Delamare-Deboutville et al., 2019). Otherwise, the study of an enriched community is also useful to elucidate which are the most adequate species to perform the process if pure cultures are used for generating a target product, such as food-related products (which higher market price than feed), or feed products in countries with restrictive legislations would not allow using mixed cultures. To the best of our knowledge, the potential of an enriched PPB community (without requiring axenic conditions) growing photoautotrophically on H₂ as SCP source remains unexplored. The effect of abiotic operating conditions on yields and H₂ uptake rates have never been assessed.

In this study, the use of an enriched PPB consortia for the bioconversion of H₂ into SCP has been assessed. The influence of environmental conditions (*i.e.*, temperature, pH and light intensity) on microbial growth kinetics, biomass characteristics, protein contents, and bacterial populations, has been evaluated. A mechanistic model has also been developed to represent the H₂ uptake process and to determine the specific H₂ uptake rates under different environmental conditions.

2. Materials and methods

2.1. Mineral salt medium and reagents

The mineral salt medium (MSM) was composed of ($\text{g}\cdot\text{L}^{-1}$): 4.2 NaHCO_3 , 4.0 KH_2PO_4 , 0.4 NH_4Cl , 0.2 $\text{MgSO}_4\cdot 7\text{H}_2\text{O}$, 0.075 $\text{CaCl}_2\cdot 2\text{H}_2\text{O}$, 0.02 g EDTA, 0.012 g $\text{FeSO}_4\cdot 7\text{H}_2\text{O}$, and 1 mL of trace elements solution. The trace elements solution contained ($\text{g}\cdot\text{L}^{-1}$): 2.8 H_3BO_3 , 2.5 $\text{MnCl}_2\cdot 4\text{H}_2\text{O}$, 0.75 $\text{Na}_2\text{MoO}_4\cdot 2\text{H}_2\text{O}$, 0.24 $\text{ZnSO}_4\cdot 7\text{H}_2\text{O}$ and 0.04 $\text{Cu}(\text{NO}_3)_2\cdot 3\text{H}_2\text{O}$. The medium was based on the MSM used for photoheterotrophic purple bacteria growth proposed by Ormerod et al. (1961), modified to ensure photoautotrophic growth (no organic carbon source such as acetate was added). NaHCO_3 was used as an inorganic carbon source instead of CO_2 to avoid carbon limitation due to limited gas-liquid mass transfer. KH_2PO_4 was used as buffer to avoid a pH increase above 8.5 (Spanoghe et al., (2021)). All reagents were obtained from Sigma-Aldrich (France) with a purity above 99%. Pure nitrogen ($\geq 99.999\%$) and hydrogen ($\geq 99.999\%$) were supplied by Linde France S.A.

2.2. Inoculum and autotrophic PPB enrichment

An enriched photoheterotrophic PPB culture grown in continuous photobioreactors treating wastewater was collected in Madrid (Spain) and used as a pre-inoculum. A series of batch enrichments in 500 mL Schott flasks were performed to obtain a PPB consortium able to provide a stable photoautotrophic growth. Stable performance was considered to be achieved when consistent results, i.e. similar biomass yields, COD and N contents in the biomass, and consistent time spans needed to attain pressures below 1.0 bar, were observed over five consecutive enrichment cycles. During each enrichment, aliquots of 20 mL from the previous culture were added into Schott flasks with 230 mL of fresh medium. The bottles were closed and the headspace was flushed with N_2 to minimize the presence of O_2 and ensure anaerobic conditions. Then, the headspace was flushed with H_2 for 2-3 min and H_2 was supplied to

reach an initial headspace pressure of ~1.3 bar, to increase the gas-liquid mass transfer without exceeding the maximum safe pressure in the flasks (1.5 bar). The flasks were incubated under continuous illumination at $\sim 50 \text{ W}\cdot\text{m}^{-2}$, using infrared LED lights (850 nm; INSTAR IN-905, Germany). The flasks were covered with an UV/VIS absorbing foil (Lee filter ND 1.2 299) to prevent the growth of competitors, such as microalgae, by minimizing the input of visible light (Capson-Tojo et al., 2021). A temperature of $25\pm 4 \text{ }^\circ\text{C}$ was maintained. The enrichments were grown under continuous magnetic agitation at 600 rpm. The headspace pressure was monitored daily. Once the pressure dropped below 1.0 bar, hydrogen was added again to reach 1.3 bar. In addition, 2 mL of liquid sample were withdrawn twice a day to monitor biomass growth by optical density (OD), measured at 660 nm and 808 nm according to the wavelengths applied previously to follow PPB mixed consortium growth (Hülßen et al., 2014; Sepúlveda-Muñoz et al., 2020). However, the OD curves did not correlate consistently with the volatile suspended solids concentrations, as they varied considerably between consecutive enrichments (probably due to different pigment composition and contents, Supplementary Material). For this reason, the use of OD for following biomass growth was discarded. Total and soluble COD concentrations were measured instead. Each enrichment batch lasted for around one week. After this time, an aliquot was taken and the procedure was restarted. A total of 14 cycles were carried out to ensure that the obtained inoculum showed consistent performances in terms of biomass yields. Photoheterotrophic enrichments, using $0.47 \text{ g}\cdot\text{L}^{-1}$ of acetate as a carbon source, instead of bicarbonate, and $0.02 \text{ g}\cdot\text{L}^{-1}$ of yeast extract according to Ormerod et al. (1961), were also performed for comparison purposes. Absorption spectra (300-1000 nm) of autotrophic and heterotrophic enrichments were also determined.

2.3. Influence of environmental conditions on autotrophic PPB grow and protein production

Once the enrichment was stable and showed a constant performance in terms of yields and nutrients consumption, batch assays at two different stirring speeds of 150 and 600 rpm were run to evaluate different gas-transfer kinetics and to corroborate that, at 600 rpm, the limiting factor was not the H₂ gas-liquid mass transfer. A similar experimental setup as for the enrichments was used (see Section 2.2). The working volume of the flasks was decreased down to 200 mL (190 mL of MSM and 10 mL of enriched PPB consortium with an initial biomass concentration in terms of volatile suspended solids of $0.11 \pm 0.02 \text{ g} \cdot \text{L}^{-1}$) to increase the volume of H₂ in the headspace and thus the interface surface to liquid volume ratio, favouring H₂ transfer from the gas to the liquid phase. The stirring speed was fixed at 600 rpm and the influence of environmental conditions (e.g., initial pH, temperature and light intensity) on the batch performance was tested. Autotrophic batch assays at initial pH values of 6, 7 and 8.5, temperatures of 15, 25, 38 and 50 °C, and infrared light intensities of 0, 5, 15, 30 and 50 W·m⁻² were carried out in triplicate (Figure 1). Two control assays, one without light and one without H₂ were also conducted under equivalent conditions. The gas composition and the pressure in the flask headspace were monitored 4-5 times per day. Gas composition changed over time due to biological uptake. The headspace was not only composed of H₂, but also of some CO₂ that was stripped from the MSM and of trace concentrations of N₂. These data were used to calculate H₂ consumption rates and overall H₂ consumption. In these assays, hydrogen was added twice: initially until an initial pressure of ~1.3 bar, and once again when the pressure dropped below 1.1 bar (based on previous unpublished results), trying to avoid H₂ limitation as well as operating at negative pressures in the flasks. Liquid samples were drawn at the beginning and end of each assay to determine biomass yields and productivities, crude protein contents, amino acid profiles and to study the microbial communities. In addition, 2 mL of liquid sample were drawn twice a day to follow the pH evolution. The experiments

lasted for 2.2-2.3 days (until the second H₂ injection was consumed and the pressure dropped again to around 1.1 bar).

<Figure 1>

2.4. Analytical procedures and microbial analysis

The physical-chemical analyses were performed at the Bio2E platform (Bio2E INRAE, 2018). Gas composition (H₂, CO₂, O₂ and N₂) was determined using a GC Perkin Clarus 580 coupled to a thermal conductivity detector and equipped with the following columns: a RtUBond (30 m × 0.32 mm × 10 μm) and a RtMolsieve (30 m × 0.32 mm × 20 μm), both with argon (31.8 mL·min⁻¹) as the carrier gas at 350 kPa. The ambient and cultivation temperatures were monitored every minute using a temperature sensor PT 100 (Jumo, Germany). Incident light intensity was measured at the beginning of each experiment by an Ocean HDX spectrophotometer (Ocean Optics, USA). The pressure inside the bottles was monitored using a manual pressure sensor LEO2 (Keller, Switzerland). The pH was monitored using a FiveGo F2 pHmeter (Mettler Toledo, Switzerland). Concentrations of total and volatile suspended solids (TSS and VSS) and total Kjeldahl nitrogen (TKN) were determined according to standard methods (Eaton et al., 2005). Concentrations of total and soluble COD were measured using an Aquamatic 420721 COD Vario Tube Test LR (0-150 mg·L⁻¹) and MR (0-1500 mg·L⁻¹). Dissolved N-NH₄⁺ concentrations were determined following sample filtration through a 0.22 μm pore size filter (as for soluble COD), using a Gallery Plus sequential analyser (Thermo Fisher, USA). The elemental composition of the PPB biomass (C, N and H contents) was determined using a LECO CHNS-932 analyser (LECO, Italy). Amino acid profiles were analysed from nine chosen samples. Four samples from the enrichments were chosen to confirm the robustness of the consortium. The rest of the samples allowed to study the impact of the pH (6, 7 and 8.5), temperature (25 and 38 °C) and light intensity (15 and 50 W·m⁻²) on the amino acid profiles. These analyses were carried out at the Biological Research

Centre of the Spanish National Research Council (Madrid, Spain). Liquid samples for amino acid analysis were dried using a speed vacuum. After that, these samples were hydrolysed by the addition of 200 μ L of 6 N HCl and a phenol crystal and kept at 110 °C during 21 h. Then, samples were dried again by vacuum and were then re-dissolved in a loading buffer (citrate at pH 2.2) before their analysis in an ion exchange chromatography column (Biochrom 30 series Amino Acid Analyser; Biochrom Ltd., United Kingdom). Absorption spectra were measured using a SPARK® multimode microplate reader (Tecan, Switzerland). Dissolved oxygen (DO) was measured using a FDO™ 925 oximeter (WTW, Germany).

The structure of the bacterial communities from the same nine samples used for amino acid analyses were also studied via 16S rRNA sequencing. The centrifuged biomass was used for DNA extraction by means of the FastDNA SPIN kit for soil following manufacturer's instructions (MP biomedical, LCC, California, USA). Sequencing of the extracted DNA was done at the GeT PlaGe sequencing centre of the Genotoul life science network (Toulouse, France). The V3-V4 regions of the 16S rRNA gene were amplified by PCR using universal primers (forward primer CTTTCCCTACACGACGCTCTTCCGATCTTACGGRAGGCAGCAG and reverse primer GGAGTTCAGACGTGTGCTCTTCCGATCTTACCAGGGTATCTAATCCT, as in Carmona et al. (2015)), the amplification products were verified by a 2100 Bioanalyzer (Agilent, USA). Then, the libraries were loaded onto the Illumina MiSeq cartridge for sequencing using a 2 x 300 pb paired-end run. The raw sequences obtained were analysed using bioinformatic tools. Mothur v.1.48.0 was used for reads cleaning, paired-ends joining and quality checking. SILVA release 132 was used for alignment and taxonomic outline.

2.5. Calculations and statistical analysis

The volumetric H₂ mass transfer coefficients ($K_{L}a_{H_2}$) in the bottles at different stirring speeds were estimated from $K_{L}a_{O_2}$ values, obtained under the same conditions, based on their different diffusion coefficients (D) according to the Higbie model (Ndiaye et al., 2018):

$$\frac{K_{L}a_{H_2}}{K_{L}a_{O_2}} = \sqrt{\frac{D_{H_2}}{D_{O_2}}} \quad (1)$$

D values of H₂ and O₂ of $4.5 \times 10^{-5} \text{ cm}^2 \cdot \text{s}^{-1}$ and $2 \cdot 10^{-5} \text{ cm}^2 \cdot \text{s}^{-1}$, respectively at 25 °C were used (Spanoghe et al., 2021). The determination of $K_{L}a_{O_2}$ was carried out in 500 mL Schott flasks open to the atmosphere by adding 200 mL of MSM (abiotic conditions) at ~25 °C. Firstly, DO in the MSM was removed down to values below 1 mg O₂·L⁻¹ by N₂ bubbling. After that, agitation was turned on and the DO concentration was recorded every 15 s, until the saturation concentration was reached. The $K_{L}a_{O_2}$ was calculated from the slope of the linearization of DO concentration vs. time (Spanoghe et al., 2021).

Since hydrogen gas was the electron donor for the enriched PPB consortium, the biomass yield is expressed according to the consumed COD-H₂ equivalent. This biomass yield (Y) was calculated as:

$$Y(g \text{ COD} \cdot g \text{ COD}^{-1}) = \frac{([\text{COD}_{ENDT}] - [\text{COD}_{ENDS}]) \cdot V_{liq}(g \text{ COD}) - ([\text{COD}_{0T}] - [\text{COD}_{0S}]) \cdot V_{liq}(g \text{ COD})}{H_2 \text{ CONSUMPTION}(\text{mol}) \cdot 16(g \text{ COD} \cdot \text{mol}^{-1})} \quad (2)$$

where COD_{END} is the total (T) and soluble (S) COD concentrations measured in the cultivation broth at the end of the batch assays and COD₀ is the initial COD concentration. V_{liq} is the volume of liquid. H_{2consumption} represents the amount of H₂ that was consumed during the batch assays. The number of moles of H₂ at a given time was calculated using ideal gas law, as:

$$n_{H_2}(\text{mol}) = \frac{P(\text{bar}) \cdot V_h(\text{L}) \cdot \%H_2}{R(\text{L} \cdot \text{bar} \cdot \text{K}^{-1} \cdot \text{mol}^{-1}) \cdot T(\text{K}) \cdot 100} \quad (3)$$

where P is the absolute pressure, V_h is the volume of the headspace, % H₂ the percentage of H₂ in the gas, R the ideal gas constant (0.08314 L·bar·K⁻¹·mol⁻¹) and T the temperature. V_h was calculated as the difference between the total volume of the Schott flask and the volume

of the cultivation broth (MSM and inoculum) and the magnetic stirrer. The volume of the cultivation broth was determined by measuring the differences between the weight of the flasks with and without cultivation broth addition, taking into account the water density at the liquid temperature.

Biomass yields were also calculated as measured VSS mass:

$$Y(g\ VSS \cdot g\ H_2^{-1}) = \frac{([VSS_{END}] - [VSS_0]) \cdot V_{liq}(g\ VSS)}{H_2\ CONSUMPTION(mol) \cdot 2(g\ H_2 \cdot mol^{-1})} \quad (4)$$

The overall H_2 uptake rates were calculated from the slope of the linearization of cumulative H_2 consumption vs. time. The specific uptake rates were estimated by the mechanistic model developed (see section 2.6). The overall N uptake rates were calculated as the difference of the $N-NH_4^+$ concentrations at the beginning and the end of the tests, divided by the time difference between the measurements.

Biomass productivity (P) during the effective growing period (disregarding the latency and cellular death phases) was calculated as particulate COD produced:

$$P(g\ COD \cdot L^{-1} \cdot d^{-1}) = \frac{([COD_{iT}] - [COD_{i-1T}]) \cdot V_{liq}(g\ COD \cdot L^{-1}) - ([COD_{i-1T}] - [COD_{i-1S}]) \cdot V_{liq}(g\ COD \cdot L^{-1})}{t_i - t_{i-1} (d)} \quad (5)$$

where COD_i and COD_{i-1} are the total (T) and soluble (S) COD concentrations calculated at times i and $i-1$, respectively, whereas t is the time.

The crude protein content of the biomass was estimated based on TKN measurements as follows (Eding et al., 2006):

$$Crude\ Protein\ content(\%) = \frac{([TKN_T] - [TKN_S])(g\ N \cdot L^{-1}) \cdot 6.25(g\ protein \cdot g\ N^{-1})}{VSS(g \cdot L^{-1})} \cdot 100 \quad (6)$$

where TKN_T and TKN_S are the total and soluble TKN concentrations, respectively.

Protein yields and productivities were calculated from those of the biomass, as:

$$Y_{protein}(g\ protein \cdot g\ H_2^{-1}) = Y(g\ VSS \cdot g\ H_2^{-1}) \cdot protein\ content(g\ protein \cdot g\ VSS^{-1}) \quad (7)$$

$$P_{protein} (g \text{ protein} \cdot L^{-1} \cdot d^{-1}) = P (g \text{ VSS} \cdot L^{-1} \cdot d^{-1}) \cdot \text{protein content} (g \text{ protein} \cdot g \text{ VSS}^{-1}) \quad (8)$$

The results here presented are provided as average values of triplicate flasks, along with their corresponding standard deviations for measured values, and 95% confidence intervals in the case of calculated parameters. In the case of productivities, the average values were calculated with the results of different measurements obtained during the exponential phase (n=12). t-student tests or one-way ANOVAs were performed to compare between means.

2.6. Mechanistic model development and parameter estimation

A mechanistic model was developed to represent accurately the H₂ consumption process by PPB and, most importantly, to avoid biased estimations of the H₂ uptake rates due to physical gas-transfer rate limitations (not biological). The developed model considered photoautotrophic growth of PPB as the main biological process, together with biomass death. Gas-liquid mass transfer kinetics were considered for both H₂ and CO₂, as in Capson-Tojo et al. (2023). This is crucial for modelling gas-fed processes, as models must account for rate limitation by mass transfer due to the low solubility of gaseous substrates.

The proposed model is based on previous PPB modelling work (Capson-Tojo et al., 2023; Puyol et al., 2017a), being compatible with the IWA ADM1 and ASM series, following the IWA Benchmark (Batstone et al., 2002; Jeppsson et al., 2006). The Petersen Matrix for the model can be found in the Supplementary Material, as well as a table with the values used for the required parameters. Rates were calculated assuming Monod kinetics for biological reactions. Physiochemical rates were implemented as in Batstone et al. (2002). MATLAB (MATLAB R2021a, The MathWorks Inc., Natick, MA, USA) was used for model implementation. The codes corresponding to the developed model and the run file can be found in GitHub (<https://github.com/GabrielCapson/PPBauto>).

Calibration of kinetic parameters (i.e., maximum specific hydrogen uptake rates (k_{m,H_2}) and saturation constants (K_{S,H_2})) was performed by minimization of the residual sum of squares (lsqcurvefit in MATLAB). The variable chosen for parameter calibration was the concentration of biomass in the liquid, calculated according to the measured yields and the hydrogen consumed from the headspace. The 95% confidence intervals and the corresponding parameter uncertainties were calculated based on two-tailed t-tests from the standard error of the parameter (nlparci function).

As in Capson-Tojo et al. (2023) and (2022), the impact of temperature and light intensity on the estimated k_{m,H_2} values was modelled according to the cardinal temperature model with inflexion (CTMI; (Ruiz-Martínez et al., 2016)) and the Steele's equation (Wágner et al., 2018), respectively. The results were fitted to these equations also via minimization of the sum of squares.

3. Results and discussion

3.1. PPB enrichments

A total of 14 enrichment cycles were carried out. H_2 consumption was detected from the third cycle onwards, confirming the ability of the mixed PPB culture for growing photoautotrophically. Biomass yields of $0.96 \pm 0.02 \text{ g COD}_{\text{biomass}} \cdot \text{g COD}_{\text{consumed}}^{-1}$ were obtained consistently during the last five enrichments, which allowed us to assume that the developed enrichment had reached a stable performance. Results of 16S rRNA gene sequencing confirmed this (see Section 3.4). These biomass yields are in agreement with those achieved during photoheterotrophic growth for both pure and enriched PPB cultures ($0.9\text{-}1.1 \text{ g COD}_{\text{biomass}} \cdot \text{g COD}_{\text{consumed}}^{-1}$) (Capson-Tojo et al., 2020). These values correspond to $6.8 \pm 0.9 \text{ g VSS} \cdot \text{g H}_{2\text{consumed}}^{-1}$, also in agreement with those obtained for pure PPB cultures grown autotrophically ($5.1\text{-}7.8 \text{ g TSS} \cdot \text{g H}_{2\text{consumed}}^{-1}$) (Spanoghe et al., 2021). Average COD

contents in the biomass (showing the degree of biomass reduction) of $1.29 \pm 0.15 \text{ g COD}_{\text{biomass}} \cdot \text{g VSS}^{-1}$ were obtained during the last five enrichment cycles, further confirming the culture stability. These values were slightly lower than those obtained in the parallel heterotrophic enrichment ($1.48 \pm 0.10 \text{ g COD}_{\text{biomass}} \cdot \text{g VSS}^{-1}$) and those previously reported for PPB with heterotrophic growth ($1.35\text{-}1.96 \text{ g COD}_{\text{biomass}} \cdot \text{g VSS}^{-1}$) (Alloul et al., 2019; Hülsen et al., 2020), but comparable with the degree of biomass reduction commonly reported for activated sludge biomass ($1.2\text{-}1.6 \text{ g COD}_{\text{biomass}} \cdot \text{g}^{-1} \text{ VSS}$) (Bullock et al., 1996). A stable N content ($143 \pm 19 \text{ mg N} \cdot \text{g VSS}^{-1}$) was also observed during the last five enrichments. Similar N proportions ($165 \pm 30 \text{ mg N} \cdot \text{g VSS}^{-1}$) were observed in the heterotrophic reactor growing in parallel.

Results from 16S rRNA gene sequencing from samples taken from the cycles of enrichments seven, thirteen and fourteen confirmed that the consortium was stable and dominated by PPB (>83%), with *Rhodobacter* sp. and *Rhodospirillum rubrum* sp. as dominant genera (see Section 3.4). In addition, absorption spectra measurements (Supplementary Material) showed typical absorption peaks of PPB cultures confirming the presence of common pigments in PPB cultures, such as bacteriochlorophylls a and b.

3.2. Impact of environmental conditions on overall rates and biomass yields

No biomass growth nor H_2 consumption were observed under the absence of light or H_2 . Environmental conditions had a noticeable impact on H_2 consumption kinetics (Figure 2, Table 1). Overall H_2 consumption rates of 35 ± 1 , 58 ± 7 and $14 \pm 1 \text{ mg COD}_{\text{H}_2\text{consumed}} \cdot \text{d}^{-1}$ were obtained at initial pH values of 6, 7 and 8.5, at temperatures of $25 \pm 4 \text{ }^\circ\text{C}$ and a light intensity of $50 \text{ W} \cdot \text{m}^{-2}$. Therefore, the optimum initial pH was 7, which increased up to 8.4 at the end of the experiment due to CO_2 consumption. The overall H_2 consumption rates were lower at both initial pH values of 6 (final pH of 6.3) or 8.5 (final pH of 9.0) (Figure 2a). The latter resulted in the lowest overall H_2 consumption rates. Initial pH values of 7 have been reported as

optimum for hydrogen production by heterotrophic PPB consortia (Capson-Tojo et al., 2020; Lazaro et al., 2015). pH values between 6 and 8.5 have been reported as appropriate for the heterotrophic growth of PPB such as *Rhodospseudomonas palustris* (van Niel, 1944), but values of 8.5 and higher have been found to decrease hydrogen yields and growth rates (Capson-Tojo et al., 2020). Regarding temperature (initial pH of 7 and light intensity of 50 $\text{W}\cdot\text{m}^{-2}$), the most favourable value for H_2 uptake by PPB was 25 °C, decreasing from overall uptake rates of $58\pm 7 \text{ mg COD}_{\text{H}_2\text{consumed}}\cdot\text{d}^{-1}$ to values of $37\pm 3 \text{ mg COD}_{\text{H}_2\text{consumed}}\cdot\text{d}^{-1}$ at a temperature of 38 °C. Although the increase in the temperature from 25 °C to 38 °C did not entail an increase in the H_2 consumption rates by PPB, the use of an inoculum previously acclimated to 38 °C could have improved H_2 consumption under this condition. Negligible H_2 consumption was recorded at 50 °C due to growth inhibition. Finally, a decrease in the overall H_2 uptake rate down to $10\pm 3 \text{ mg COD}_{\text{H}_2\text{consumed}}\cdot\text{d}^{-1}$ was also observed when the temperature was decreased down to 15 °C, despite a higher H_2 solubility in the cultivation broth, indicating lower biological uptake rates. Similar optimal ranges were reported by Capson-Tojo et al. (2023) for enriched purple phototrophic bacteria cultures grown photoheterotrophically. In agreement, Hülsen et al. (2016) reported higher PPB heterotrophic growth rates at a temperature of 30 °C compared to 10 °C, with a drop of 20% in PPB activity. This study confirmed a higher relative tolerance to higher temperatures than to lower values, since the decrease in rates at 38 °C was less pronounced than at 15 °C (using an inoculum acclimated to 25 ± 4 °C). Concerning light intensities (initial pH of 7 and temperature of 25 ± 4 °C), light limitation was observed at intensities lower than $30 \text{ W}\cdot\text{m}^{-2}$, whereas similar overall rates were measured at both 30 and $50 \text{ W}\cdot\text{m}^{-2}$, with values of 61 ± 5 and $58\pm 7 \text{ mg COD}_{\text{H}_2\text{consumed}}\cdot\text{d}^{-1}$, respectively. This minimum threshold needed to achieve the maximum H_2 uptake rate was similar to that estimated by Capson-Tojo et al. (2022) using acetate as substrate for PPB growth. An optimum light intensity of 30-100 $\text{W}\cdot\text{m}^{-2}$ has been previously reported for the

production of H_2 by heterotrophic PPB (Li and Fang, 2009). In a real scale, the use of sunlight as a free energy source would be mandatory to reduce capital and operating costs (Capson-Tojo et al., 2020). Under these outdoor conditions, the use of a low-cost UV/VIS filter can limit the growth of PPB competitors (Hülßen et al., 2022c).

Overall $N-NH_4^+$ consumption rates of $23 \pm 5 \text{ mg } N_{\text{consumed}} \cdot L^{-1} \cdot d^{-1}$ were obtained under the optimal conditions of initial pH of 7, temperature of $25 \pm 4 \text{ }^\circ\text{C}$ and a light intensities $> 30 \text{ W} \cdot m^{-2}$. In this respect, taking into account an initial $N-NH_4^+$ concentration in the cultivation broth of $\sim 105 \text{ mg } N \cdot L^{-1}$, the PPB growth was not limited by N (confirmed by minimal residual $N-NH_4^+$ concentrations at the end of the tests of $44 \text{ mg } N \cdot L^{-1}$). Inorganic C consumption rates could not be reported due to measurement errors induced by equipment sensitivity and initial CO_2 stripping.

<Figure 2>

<Table 1>

In agreement with the H_2 consumption rates, the biomass productivities were also affected by the environmental conditions (Figure 3). Average biomass productivities decreased from 351 ± 36 to $202 \pm 23 \text{ mg } COD \cdot L^{-1} \cdot d^{-1}$ when the initial pH was decreased from 7 to 6 (at $25 \text{ }^\circ\text{C}$ and a light intensity of $50 \text{ W} \cdot m^{-2}$). The decrease was even more significant ($p < 0.05$) at pH 8.5, with average biomass productivities of $77 \pm 16 \text{ mg } COD \cdot L^{-1} \cdot d^{-1}$ under the same temperature and illumination conditions. Compared to $25 \text{ }^\circ\text{C}$, lower biomass productivities of 56 ± 28 and $182 \pm 36 \text{ mg } COD \cdot L^{-1} \cdot d^{-1}$ were obtained at $15 \text{ }^\circ\text{C}$ and $38 \text{ }^\circ\text{C}$, respectively. No significant differences ($p > 0.05$) between biomass productivities were obtained under no light limitation (50 and $30 \text{ W} \cdot m^{-2}$), whilst the reduction of the light intensity to 15 and $5 \text{ W} \cdot m^{-2}$, resulted in a 71% and 83% decrease in productivities. The maximum average biomass productivities hereby achieved with the enriched PPB culture (of $380 \text{ mg } COD \cdot L^{-1} \cdot d^{-1}$;

corresponding to $0.31 \text{ g VSS}\cdot\text{L}^{-1}\cdot\text{d}^{-1}$) were slightly higher than those reported for pure photoautotrophic PPB cultures ($\sim 0.25 \text{ g TSS}\cdot\text{L}^{-1}\cdot\text{d}^{-1}$), also obtained in batch reactors (Spanoghe et al., 2021). Moreover, these results are comparable to those from non-axenic photoheterotrophic PPB growth under batch, fed-batch and continuous reactors (Capson-Tojo et al., 2020). However, the maximum biomass productivities were 6-times lower than those achieved by aerobic HOB in sequencing batch reactors (Matassa et al., 2016b). These lower biomass productivities with PPB are mostly a consequence of the generally faster kinetics of aerobic processes, thanks to the highly efficient energy utilization when oxygen is the final electron acceptor (Schmidt-Rohr, 2020). In addition, the mode of cultivation of PPB in the presence of light as compared to other non-phototrophic microorganisms might also lead to different productivities. Although PPB exhibit lower biomass productivities compared with HOB, the high biomass yields in PPB might compensate this drawback. The biomass productivities were also approximately 2-times lower than those obtained for pure photoheterotrophic PPB cultures operating in batch mode (Capson-Tojo et al., 2020). Nevertheless, batch durations or biomass concentrations were not optimized here, so higher values can be expected from continuous reactors.

<Figure 3>

Similar overall biomass yields ($0.99\pm 0.04 \text{ g COD}_{\text{biomass}}\cdot\text{g COD}_{\text{consumed}}^{-1}$) were obtained regardless of the environmental conditions tested in this study (Table 1). These yields corresponded to $7.7\pm 0.5 \text{ g VSS}\cdot\text{g H}_{2\text{consumed}}^{-1}$, a value higher than those reported for pure cultures of *Rhodobacter capsulatus* and *Rhodobacter sphaeroides* ($5.1\text{-}6.7 \text{ g TSS}\cdot\text{g H}_{2\text{consumed}}^{-1}$), and similar to *Rhodospseudomonas palustris* (Spanoghe et al., 2021). The fact that high yields could be maintained using PPB enriched cultures is promising for the scale up of this process, since the costs of axenic conditions are prohibitive at full-scale installations (at least when resource recovery is considered). In addition, the high substrate to biomass conversion

is a key benefit compared with other microorganisms such as HOB for SCP production. Average biomass yields of $0.2 \text{ g COD}_{\text{biomass}} \cdot \text{g COD}_{\text{consumed}}^{-1}$ have been reported for a HOB enrichments using ammonium as N source as in this study (Hu et al., 2020). Maximum biomass yields of 1.3 and $2.3 \text{ g VSS} \cdot \text{g H}_{2\text{consumed}}^{-1}$ have been obtained for an enrichment of HOB under batch and continuous operation mode, respectively (Matassa et al., 2016a). In this context, the use of PPB instead of HOB could increase in almost 3-fold the production of SCP for a given amount of H_2 . In comparison, aerobic methanotrophs have biomass yields of 0.26- $0.79 \text{ g VSS} \cdot \text{g}^{-1} \text{ CH}_{4\text{consumed}}$, which correspond to values of $0.07\text{-}0.20 \text{ g VSS} \cdot \text{g COD}_{\text{consumed}}^{-1}$, much lower than for PPB ($0.96 \pm 0.06 \text{ g VSS} \cdot \text{g COD}_{\text{consumed}}^{-1}$) (Tsapekos et al., 2019; Valverde-Pérez et al., 2020). PPB growth using hydrogen as an electron donor is 4.3 times more efficient than aerobic methanotrophs in terms of COD conversion into bacterial biomass. This is explained by the total conversion of COD into biomass by PPB (using light as energy source), compared to the utilization of methane (a strongly bonded molecule) as both C and energy source by methanotrophs.

3.3. Impact of environmental conditions on biomass composition and overall protein yields and productivities

The elemental PPB biomass composition remained constant regardless the pH, temperature and light intensity (Table 1). The average C, N and H contents of the biomass (on a dry weight basis) were $42 \pm 2\%$, $9 \pm 1\%$ and $6 \pm 0\%$, respectively. Based on these values, the empirical formula of the biomass was $\text{CH}_{1.71}\text{N}_{0.18}$. Despite similar N contents (8-12% N), the C and H contents of PPB growing under autotrophic conditions were lower than those previously reported for heterotrophic PPB growth, of 52-55% C and 8-9% H (Carlozzi et al., 2006; Sepúlveda-Muñoz et al., 2022). Despite these lower contents, the C:H ratio remained similar (around 6) to those obtained during heterotrophic growth. More research is needed to further clarify the lower C and H content in the PPB biomass under autotrophic conditions.

According to the TKN contents in the biomass (Table 1), average crude protein yields of 4.2 ± 0.6 and 3.9 ± 0.8 g protein·g $H_{2\text{consumed}}^{-1}$ were obtained at initial pH values of 7 and 8.5, respectively (at 25 °C and $50\text{ W}\cdot\text{m}^{-2}$). In agreement with the biomass yields, a negligible impact of pH in the crude protein yields was observed in this pH range. Similarly, no significant differences ($p>0.05$) were found between the crude protein yields obtained at different temperatures (4.4 ± 1.4 , 4.2 ± 0.6 and 4.3 ± 1.2 g protein·g $H_{2\text{consumed}}^{-1}$ at 15, 25 and 38 °C, respectively) and different light intensities (4.0 ± 0.3 , 4.4 ± 1.3 and 4.2 ± 0.6 g protein·g $H_{2\text{consumed}}^{-1}$ at 15, 30 and $50\text{ W}\cdot\text{m}^{-2}$, respectively). This was expected, as both the biomass yields and the crude protein contents were similar. These values confirm the robustness of the consortia under different environmental conditions, with a crude protein content in the PPB biomass higher than 50% (Table 1). These values of crude protein contents may have been slightly overestimated since the factor 6.25 is not always representative of actual protein contents (François Mariotti and Mirand, 2008). In this respect, the amino acid concentration in selected samples analyzed was between 32-62% lower than the crude protein content. This difference was attributed to the overestimation of the factor 6.25 but also to the non-determination of certain amino acids, underestimating total protein contents. The crude protein yields obtained in this study using an enriched autotrophic PPB consortia were 1.5-fold higher than those reported for pure autotrophic PPB cultures ($2.6\text{-}2.9$ g protein·g $H_{2\text{consumed}}^{-1}$) at pH below 8, 28 °C and a light intensity of $18\text{ W}\cdot\text{m}^{-2}$. As for the biomass yields, the crude protein yields in this study were also higher than those reported for HOB, assuming a 71% protein content in the biomass (maximum values of 0.9 and 1.6 g protein·g $H_{2\text{consumed}}^{-1}$) (Matassa et al., 2016b). Lower protein yields were also reported for methanotrophic bacteria, taking into account the lower biomass yield aforementioned and the lower protein content in the biomass (around 41%) (Tsapekos et al., 2019). Protein productivities of 0.18 ± 0.02 and 0.04 ± 0.01 g protein·L⁻¹·d⁻¹ were obtained at pH values of 7 and 8.5, respectively. Although

analogous crude protein contents in the biomass were achieved at pH 8.5, the lower protein productivity at this pH was a result of the lower biomass productivities. Protein productivities also decreased to 0.10 ± 0.02 and 0.04 ± 0.02 g protein·L⁻¹·d⁻¹ at 38 °C and 15 °C, respectively. Similar protein productivities were obtained at 50 and 30 W·m⁻², while a decrease in the light intensity to 15 W·m⁻² led to a decrease in the protein productivities down to 0.03 ± 0.02 g protein·L⁻¹·d⁻¹. The maximum protein productivities (0.20 g protein·L⁻¹·d⁻¹) are higher than those reported for pure autotrophic PPB cultures (0.09 - 0.12 g protein·L⁻¹·d⁻¹) (Spanoghe et al., 2021). However, the productivities were lower than those achieved by PPB consortia growing under heterotrophic conditions (0.29 - 0.64 g protein·L⁻¹·d⁻¹) (Alloul et al., 2019; Hülsen et al., 2022c) and those from HOB (0.27 g protein·L⁻¹·d⁻¹) (Matassa et al., 2016b). As mentioned previously, the overall productivities given here are far from being optimal. Higher values will be obtained in continuous reactors working at optimal retention times and feeding rates.

Total amino acid contents on a dry basis in the PPB biomass of $42\pm 2\%$, 35% and 20% were obtained from the autotrophic enrichments (4 samples), from samples drawn from bioreactors operating under optimal conditions (25°C , pH of 7 and light intensity of 50 W·m⁻²) and from samples from bioreactors with a low performance (pH of 6), respectively (more information in the Supplementary Material). The stable biomass composition in terms of amino acid and protein contents during the enrichments and efficient conditions underline the suitability of using biomass derived from a PPB mixed community for the production of animal feed. The maximum total amino acid content in the PPB biomass was lower than that of fishmeal but similar to soybean meal (72% and 40% , respectively). The biomass contained all essential amino acids (Figure 4; it must be considered that tryptophan was not measured), representing approximately 40% of the total amino acids under most conditions. Similar proportions of essential amino acids are found in important protein sources for feed such as soybean meal

and fishmeal, and in the biomass of pure strains of *Rhodobacter capsulatus*, *Rhodobacter sphaeroides* and *Rhodopseudomonas palustris* under autotrophic growth (FAO, 1981; Spanoghe et al., 2021). Glutamic acid, aspartic acid, alanine and leucine were the predominant amino acids in PPB biomass, accounting for more than 8% of the total amino acid content. Similarly, glutamic acid+glutamine and aspartic acid+asparagine are the most abundant amino acids in soybean meal and fishmeal. Compared to fishmeal, PPB biomass was deficient in all amino acids (Figure 4). In agreement, the PPB biomass from poultry and red meat processing wastewater exhibited also lower contents of almost all amino acids compared to fishmeal (Hülsemann et al., 2018). Otherwise, the amino acid profile of the autotrophic PPB biomass was comparable to that of soybean meal, except for glutamic acid and cystine, which were more abundant in soybean meal, and alanine, which was more abundant in PPB biomass. These results highlight the potential of PPB biomass to replace commercial protein meals. The capital/operating costs would need to be balanced out with a high product cost such as food-related products or high-value feed for making the process economically feasible. Specifically, although the amino acid content of the biomass was lower than that of fishmeal, the potential application of the PPB mixed culture biomass would be as a partial substitute of fishmeal since its market price is higher ($2 \text{ € kg}^{-1}_{\text{protein}}$) than the one of soybean meal ($0.7 \text{ € kg}^{-1}_{\text{protein}}$) (Alloul et al., 2021a; Hülsemann et al., 2022a). In this regard, the application of PPB biomass as a substitute for feed for aquaculture species has been previously demonstrated in diverse species (Alloul et al., 2021b; Delamare-Deboutteville et al., 2019).

<Figure 4>

3.4. Impact of environmental conditions on the microbial communities

The microbial analyses corroborated the development of an autotrophic PPB community, with relative abundances over 0.8 in the reactors working efficiently (Figure 5). The inoculum of

the first autotrophic enrichment (a heterotrophic PPB enriched culture) was composed mainly of the PPB genus *Rhodobacter* (81%) along with the PPB genus *Rhodopseudomonas* (2%) and non-phototrophic bacteria such as *Acinetobacter* sp. (9%) and *Cloacibacterium* sp. (4%). As for the inoculum, the main PPB genera under autotrophic growth were *Rhodobacter* sp., with a maximum relative abundance of 75% and *Rhodopseudomonas* sp. (up to 42%). *Rhodocista* sp. was another PPB genus detected in a minor proportion. Specifically, the dominant species were *Rhodobacter capsulatus* (99% similarity according to the NCBI 16S rRNA database), *Rhodobacter sphaeroides* (99%), *Rhodobacter sediminis* (99%) and *Rhodopseudomonas palustris* (99%). Most of these PPB species are known to perform photoautotrophic growth using hydrogen as electron donor (Spanoghe et al., 2021). The same PPB species are also typically reported as dominant during the treatment of different types of wastewaters (heterotrophic growth) (Alloul et al., 2019; Capson-Tojo et al., 2021; Hülsen et al., 2022b, 2014). This suggests that most commonly known photoheterotrophic PPB are also those having the competitive advantage in mixed cultures during autotrophic growth.

Rhodobacter sp. was the predominant PPB genus during most of the enrichments and batch experiments used to screen the operational parameters except for the test at 38 °C, where the *Rhodopseudomonas* sp. abundance increased and became dominant. In this regard, Hülsen et al. (2020) reported a population shift from *Rhodopseudomonas* sp. towards *Rhodobacter* sp. due to the decrease in the batch duration from 3 to 2 days, but the correlation between the batch duration and the relative abundance of *Rhodopseudomonas* sp. was far from conclusive and the observation could not be repeated. Other articles have reported the opposite effect, with *Rhodobacter* sp. dominating at short retention times and *Rhodopseudomonas* sp. at longer times (Alloul et al., 2019). Therefore, the batch duration was discarded as potential explanation for the dominance of *Rhodobacter* sp. in our reactors. In addition, the duration of the batch enrichments was around one week and the predominant genus in those was also

Rhodobacter sp. Otherwise, the predominance of *Rhodopseudomonas* sp. at 38 °C could be explained as a proliferation due to a high temperature tolerance. *Rhodopseudomonas palustris* (the most similar strain in this study, 99%) indeed presented superior growth under temperatures between 35-40 °C than at 30 °C (du Toit and Pott, 2021). Nevertheless, the impact of the environmental and operational conditions on *Rhodobacter-Rhodopseudomonas* interactions in PPB-enriched cultures is far from clear, and more research needs to be done using dedicated co-cultures.

The remaining genera detected corresponded mostly to anaerobic fermenters such as *Cloacibacterium* sp., *Paludibacter* sp., *Acholeplasma* sp. and *Dysgonomonas* sp., and to a lesser extent, to aerobic bacteria such as *Chryseobacterium* sp. and *Acinetobacter* sp. Despite the anaerobic conditions in the enrichments, the presence of air during the transport of the inoculum and/or during the enrichment preparation could justify the presence of these bacteria. Most of these genera were also found in previous mixed PPB consortia growing heterotrophically (Alloul et al., 2019). An increase in the proportions of anaerobic fermenters, mainly the genera *Cloacibacterium* sp. and *Dysgonomonas* sp. was observed under non-optimal conditions (pH 6 and 8.5 and light intensity of 15 W·m⁻²). *Cloacibacterium* sp. was the most abundant fermenter at pH 6, while *Dysgonomonas* sp. was favoured by neutral-alkaline pH values. The decline in the abundance of PPB could be attributed to a lesser growth extent, resulting in higher proportions of fermenters. Efficient continuous operation should be able to reduce the presence of both fermenters and aerobic bacteria in the reactors. As a result, a higher abundance of PPB and a more stable population would be expected in an optimized system thanks to the specific conditions applied in the process (i.e. anaerobic conditions, H₂ as a COD source, and near-infrared light as light source).

<Figure 5>

3.5. Modelling autotrophic PPB growth: estimation of specific uptake rates

The model was calibrated by minimization of the residual sum of squares using the concentration of biomass in the liquid as experimental data. Figures in the Supplementary Material show, as examples, the results for one of the batch tests, mixed at 150 rpm. The results show that the model predicted accurately the experimental behaviour, with R^2 values from Pareto plots for biomass and hydrogen gas concentrations of 0.995 and 0.900, respectively. Despite the change in limiting rates throughout the batch test, the model was able to represent the whole process. Before 0.9-1.0 d, H_2 was sufficient, and consumption rates were limited by biological uptake (typical exponential curve, soluble H_2 concentrations higher than saturation constants for H_2 (K_{S,H_2} ; below $0.05 \text{ mg COD}\cdot\text{L}^{-1}$ in all the tests performed) and the calculated uptake rates increased with supply rates). After 0.9-1.0 d, the H_2 transfer rate became limiting due to the high biomass concentrations and the low H_2 K_{La} (28.7 d^{-1} in this test), a situation that did not change despite the injection of extra H_2 in the headspace. After this point, the concentration of H_2 in the liquid was always close to zero, the growth curve became linear and the uptake rate was limited by the transfer rate. The model predicted accurately this behaviour, confirming its applicability for estimating the specific uptake rates. It must be considered that, at the moment, the model only considers one biomass as state variable (lumped PPB; see Supplementary Material). Therefore, the shifts in PPB populations described above cannot be account for by the model. Further work should be done to study these microbial interactions, including them in coming models.

The tested environmental conditions affected considerably the H_2 specific uptake rates (Figure 6 and Table 1). In agreement with the overall rates, optimal specific rates of $1.9\text{-}2.0 \text{ g COD}\cdot\text{g COD}^{-1}\cdot\text{d}^{-1}$ were achieved at initial pH values of 7, $25 \text{ }^\circ\text{C}$, and light intensities over $30 \text{ W}\cdot\text{m}^{-2}$ (Table 1). Lower or higher pH values and temperatures resulted in decreased rates. No photoinhibition was observed at $50 \text{ W}\cdot\text{m}^{-2}$. With R^2 values of 0.97 and 0.91, the Steele's equation and the CTMI were able to represent the impacts of light intensity and temperature

accurately, respectively (Figure 6). The optimal conditions are similar to those reported for photoheterotrophic PPB growth, confirming these values and suggesting that the growth mode does not affect optimal conditions (Capson-Tojo et al., 2022, 2020). Optimal specific uptake rates of $2 \text{ g COD} \cdot \text{g COD}^{-1} \cdot \text{d}^{-1}$ are close to those for photoheterotrophic processes ($2.3\text{-}2.7 \text{ g COD} \cdot \text{g COD}^{-1} \cdot \text{d}^{-1}$ (Capson-Tojo et al., 2023; Puyol et al., 2017a) and similar to those reported for pure PPB cultures grown autotrophically (below $2.3 \text{ g COD} \cdot \text{g COD}^{-1} \cdot \text{d}^{-1}$ (Spanoghe et al., 2021)). These results show that the developed model can effectively be used to represent the process dynamics at different conditions, allowing determining potential gas-transfer limitations. The model has only been validated so far for laboratory scale batch tests. Further work will aim at further validating the model with different reactor configurations (e.g. in continuous systems) and using it to simulate different scenarios for process optimisation and efficient reactor design.

<Figure 6>

4. Conclusions

This study demonstrates the applicability of PPB enriched cultures to produce SCP using H_2 efficiently. Neutral pH, temperatures of $25 \pm 4 \text{ }^\circ\text{C}$ and light intensities higher than $30 \text{ W} \cdot \text{m}^{-2}$ were the best conditions for biomass growth for the PPB enriched consortium used here. High biomass and protein yields, up to $8.4 \text{ g VSS} \cdot \text{g H}_2^{-1}$ ($\sim 1 \text{ g COD} \cdot \text{g COD}^{-1}$) and $4.4 \text{ g protein} \cdot \text{g H}_{2\text{consumed}}^{-1}$, were reached. Amino acid contents up to 42%, with a similar profile to that of soybean meal, underline the potential of PPB biomass as a feed substitute. These results confirm the effective photoautotrophic PPB enrichment in non-sterile environments (over 81% under optimal conditions), with *Rhodobacter* sp. as the most abundant genus. The high yields and rates achieved (maximum overall H_2 uptake rates of $61 \text{ mg COD} \cdot \text{d}^{-1}$ and specific uptake rates of $2 \text{ g COD} \cdot \text{g COD}^{-1} \cdot \text{d}^{-1}$) highlight the great potential of enriched PPB cultures for H_2 valorisation, allowing to reach specific uptake rates similar to those reached in pure

PPB cultures. Further experiments should focus on the optimization of the biomass productivities and the overall uptake rates, using continuous reactors.

Acknowledgements

María del Rosario Rodero and Jose Antonio Magdalena acknowledges the NextGenerationEU Margarita Salas programme from the European Union for their research contract. The authors would like to acknowledge INRAE Bio2E Facility (Bio2E, INRAE, 2018. Environmental Biotechnology and Biorefinery Facility (<https://doi.org/10.15454/1.557234103446854E12>) where all experiments were conducted.

References

- Alloul, A., Muys, M., Hertoghs, N., Kerckhof, F.M., Vlaeminck, S.E., 2021a. Cocultivating aerobic heterotrophs and purple bacteria for microbial protein in sequential photo- and chemotrophic reactors. *Bioresour. Technol.* 319, 124192. <https://doi.org/10.1016/j.biortech.2020.124192>
- Alloul, A., Spanoghe, J., Machado, D., Vlaeminck, S.E., 2022. Unlocking the genomic potential of aerobes and phototrophs for the production of nutritious and palatable microbial food without arable land or fossil fuels. *Microb. Biotechnol.* 15, 6–12. <https://doi.org/10.1111/1751-7915.13747>
- Alloul, A., Wille, M., Lucenti, P., Bossier, P., Van Stappen, G., Vlaeminck, S.E., 2021b. Purple bacteria as added-value protein ingredient in shrimp feed: *Penaeus vannamei* growth performance, and tolerance against *Vibrio* and ammonia stress. *Aquaculture* 530, 735788. <https://doi.org/10.1016/j.aquaculture.2020.735788>
- Alloul, A., Wuyts, S., Lebeer, S., Vlaeminck, S.E., 2019. Volatile fatty acids impacting phototrophic growth kinetics of purple bacteria: Paving the way for protein production on fermented wastewater. *Water Res.* 152, 138–147.

<https://doi.org/10.1016/j.watres.2018.12.025>

Batstone, D.J., Keller, J., Angelidaki, I., Kalyuzhnyi, S. V, Pavlostathis, S.G., Rozzi, A., Sanders, W.T.M., Siegrist, H., Vavilin, V.A., 2002. The IWA Anaerobic Digestion Model No 1 (ADM1). *Water Sci. Technol.* 45, 65–73.

<https://doi.org/10.2166/wst.2002.0292>

Bertasini, D., Binati, R.L., Bolzonella, D., Battista, F., 2022. Single Cell Proteins production from food processing effluents and digestate. *Chemosphere* 296, 134076.

<https://doi.org/10.1016/j.chemosphere.2022.134076>

Bio2E INRAE, 2018. Environmental Biotechnology and Bio-refinery Platform.

<https://doi.org/10.15454/1.557234103446854E12>

Bullock, C.M., Bicho, P.A., Zhang, Y., Saddler, J.N., 1996. A solid chemical oxygen demand (COD) method for determining biomass in waste waters. *Water Res.* 30, 1280–1284.

[https://doi.org/https://doi.org/10.1016/0043-1354\(95\)00271-5](https://doi.org/https://doi.org/10.1016/0043-1354(95)00271-5)

Capson-Tojo, G., Batstone, D.J., Grassino, M., Hülsen, T., 2022. Light attenuation in enriched purple phototrophic bacteria cultures: Implications for modelling and reactor design.

Water Res. 219, 118572. <https://doi.org/10.1016/j.watres.2022.118572>

Capson-Tojo, G., Batstone, D.J., Grassino, M., Vlaeminck, S.E., Puyol, D., Verstraete, W., Kleerebezem, R., Cehnen, A., Ghimire, A., Pikaar, I., Lema, J.M., Hülsen, T., 2020.

Purple phototrophic bacteria for resource recovery: Challenges and opportunities.

Biotechnol. Adv. 43, 107567. <https://doi.org/10.1016/j.biotechadv.2020.107567>

Capson-Tojo, G., Batstone, D.J., Hülsen, T., 2023. Expanding mechanistic models to represent purple phototrophic bacteria enriched cultures growing outdoors. *Water Res.*

229, 119401. <https://doi.org/10.1016/j.watres.2022.119401>

Capson-Tojo, G., Lin, S., Batstone, D.J., Hülsen, T., 2021. Purple phototrophic bacteria are outcompeted by aerobic heterotrophs in the presence of oxygen. *Water Res.* 194,

116941. <https://doi.org/10.1016/j.watres.2021.116941>

Carlozzi, P., Pushparaj, B., Degl'Innocenti, A., Capperucci, A., 2006. Growth characteristics of *Rhodospseudomonas palustris* cultured outdoors, in an underwater tubular photobioreactor, and investigation on photosynthetic efficiency. *Appl. Microbiol. Biotechnol.* 73, 789–795. <https://doi.org/10.1007/s00253-006-0550-z>

Carmona-Martínez, A.A., Trably, E., Milferstedt, K., Lacroix, R., Etcheverry, L., Bernet, N., 2015. Long-term continuous production of H₂ in a microbial electrolysis cell (MEC) treating saline wastewater. *Water Res.* 81, 149–156. <https://doi.org/10.1016/j.watres.2015.05.041>

Ciani, M., Lippolis, A., Fava, F., Rodolfi, L., Niccolai, A., Tredici, M.R., 2019. Microbes : Food for the Future. *Foods* 13–14.

Delamare-Deboutteville, J., Batstone, D.J., Karvaak, M., Stegman, S., Salini, M., Tabrett, S., Smullen, R., Barnes, A.C., Hülsen, J., 2019. Mixed culture purple phototrophic bacteria is an effective fishmeal replacement in aquaculture. *Water Res.* X 4, 100031. <https://doi.org/10.1016/j.wroa.2019.100031>

du Toit, J.P., Pott, R.W.M., 2021. Heat-acclimatised strains of *Rhodospseudomonas palustris* reveal higher temperature optima with concomitantly enhanced biohydrogen production rates. *Int. J. Hydrogen Energy* 46, 11564–11572. <https://doi.org/10.1016/j.ijhydene.2021.01.068>

Eaton, M.A.H., Clesceri, A.D., Rice, L.S., Greenberg, E.W., Franson, A.E., 2005. *APHA: Standard Methods for the Examination of Water and Wastewater*, Centen. ed., APHA, AWWA, WEF, Washington, DC.

Eding, E.H., Kamstra, A., Verreth, J.A.J., Huisman, E.A., Klapwijk, A., 2006. Design and operation of nitrifying trickling filters in recirculating aquaculture: A review. *Aquac. Eng.* 34, 234–260. <https://doi.org/10.1016/j.aquaeng.2005.09.007>

- Ehsani, E., Dumolin, C., Arends, J.B.A., Kerckhof, F.M., Hu, X., Vandamme, P., Boon, N., 2019. Enriched hydrogen-oxidizing microbiomes show a high diversity of co-existing hydrogen-oxidizing bacteria. *Appl. Microbiol. Biotechnol.* 103, 8241–8253. <https://doi.org/10.1007/s00253-019-10082-z>
- FAO, 1981. AMINO-ACID CONTENT OF FOODS AND BIOLOGICAL DATA ON PROTEINS, 3rd ed, FAO Food and Nutrition Series. Rome.
- François Mariotti, D.T., Mirand, P.P., 2008. Converting Nitrogen into Protein—Beyond 6.25 and Jones’ Factors. *Crit. Rev. Food Sci. Nutr.* 48, 177–184. <https://doi.org/10.1080/10408390701279749>
- Hu, X., Kerckhof, F.M., Ghesquière, J., Bernaerts, K., Rookx, P., Clauwaert, P., Boon, N., 2020. Microbial Protein out of Thin Air: Fixation of Nitrogen Gas by an Autotrophic Hydrogen-Oxidizing Bacterial Enrichment. *Environ. Sci. Technol.* 54, 3609–3617. <https://doi.org/10.1021/acs.est.9b06155>
- Hu, X., Vandamme, P., Boon, N., 2022. Co-cultivation enhanced microbial protein production based on autotrophic nitrogen-fixing hydrogen-oxidizing bacteria. *Chem. Eng. J.* 429, 132535. <https://doi.org/10.1016/j.cej.2021.132535>
- Hülßen, T., Barnes, A.C., Batstone, D.J., Capson-Tojo, G., 2022a. Creating value from purple phototrophic bacteria via single-cell protein production. *Curr. Opin. Biotechnol.* 76, 102726. <https://doi.org/10.1016/j.copbio.2022.102726>
- Hülßen, T., Barry, E.M., Lu, Y., Puyol, D., Batstone, D.J., 2016. Low temperature treatment of domestic wastewater by purple phototrophic bacteria: Performance, activity, and community. *Water Res.* 100, 537–545. <https://doi.org/10.1016/j.watres.2016.05.054>
- Hülßen, T., Batstone, D.J., Keller, J., 2014. Phototrophic bacteria for nutrient recovery from domestic wastewater. *Water Res.* 50, 18–26. <https://doi.org/10.1016/j.watres.2013.10.051>

- Hülßen, T., Hsieh, K., Lu, Y., Tait, S., Batstone, D.J., 2018. Simultaneous treatment and single cell protein production from agri-industrial wastewaters using purple phototrophic bacteria or microalgae – A comparison. *Bioresour. Technol.* 254, 214–223.
<https://doi.org/10.1016/j.biortech.2018.01.032>
- Hülßen, T., Sander, E.M., Jensen, P.D., Batstone, D.J., 2020. Application of purple phototrophic bacteria in a biofilm photobioreactor for single cell protein production: Biofilm vs suspended growth. *Water Res.* 181, 115909.
<https://doi.org/10.1016/j.watres.2020.115909>
- Hülßen, T., Stegman, S., Batstone, D.J., Capson-Tojo, G., 2022b. Naturally illuminated photobioreactors for resource recovery from piggery and chicken-processing wastewaters utilising purple phototrophic bacteria. *Water Res.* 214, 118194.
<https://doi.org/10.1016/j.watres.2022.118194>
- Hülßen, T., Züger, C., Gan, Z.M., Batstone, D.J., Solley, D., Ochre, P., Porter, B., Capson-Tojo, G., 2022c. Outdoor demonstration-scale flat plate photobioreactor for resource recovery with purple phototrophic bacteria. *Water Res.* 216, 118327.
<https://doi.org/https://doi.org/10.1016/j.watres.2022.118327>
- Jeppsson, U., Rosen, C., Alex, J., Copp, J., Gernaey, K. V., Pons, M.N., Vanrolleghem, P.A., 2006. Towards a benchmark simulation model for plant-wide control strategy performance evaluation of WWTPs. *Water Sci. Technol.* 53, 287–295.
<https://doi.org/10.2166/wst.2006.031>
- Khoshnevisan, B., Tsapekos, P., Zhang, Y., Valverde-Pérez, B., Angelidaki, I., 2019. Urban biowaste valorization by coupling anaerobic digestion and single cell protein production. *Bioresour. Technol.* 290, 121743. <https://doi.org/10.1016/j.biortech.2019.121743>
- Lazaro, C.Z., Varesche, M.B.A., Silva, E.L., 2015. Effect of inoculum concentration, pH, light intensity and lighting regime on hydrogen production by phototrophic microbial

- consortium. *Renew. Energy* 75, 1–7. <https://doi.org/10.1016/j.renene.2014.09.034>
- Li, R.U.Y., Fang, H.H.P., 2009. Heterotrophic Photo Fermentative Hydrogen Production. *Crit. Rev. Environ. Sci. Technol.* 39, 1081–1108. <https://doi.org/10.1080/10643380802009835>
- Madigan, M.T., Gest, H., 1979. Growth of the photosynthetic bacterium *Rhodospseudomonas capsulata* chemoautotrophically in darkness with H₂ as the energy source. *J. Bacteriol.* 137, 524–530. <https://doi.org/10.1128/jb.137.1.524-530.1979>
- Matassa, S., Boon, N., Pikaar, I., Verstraete, W., 2016a. Microbial protein: future sustainable food supply route with low environmental footprint. *Microb. Biotechnol.* 9, 568–575. <https://doi.org/10.1111/1751-7915.12369>
- Matassa, S., Boon, N., Verstraete, W., 2015. Resource recovery from used water: The manufacturing abilities of hydrogen-oxidizing bacteria. *Water Res.* 68, 467–478. <https://doi.org/10.1016/j.watres.2015.10.028>
- Matassa, S., Verstraete, W., Pikaar, I., Boon, N., 2016b. Autotrophic nitrogen assimilation and carbon capture for microbial protein production by a novel enrichment of hydrogen-oxidizing bacteria. *Water Res.* 101, 137–146. <https://doi.org/10.1016/j.watres.2016.05.077>
- Nasseri, A.T., Amini, K.S., Morowvat, M.H., Ghasemi, Y., 2011. Single Cell Protein: Production and Process. *Am. J. food Technol.* 6, 103–116.
- Ndiaye, M., Gadoin, E., Gentric, C., 2018. CO₂ gas–liquid mass transfer and kLa estimation: Numerical investigation in the context of airlift photobioreactor scale-up. *Chem. Eng. Res. Des.* 133, 90–102. <https://doi.org/10.1016/j.cherd.2018.03.001>
- Ormerod, J.G., Ormerod, K.S., H.Gest, 1961. Light-dependent utilization of organic compounds and photoproduction of molecular hydrogen by photosynthetic bacteria; relationships with nitrogen metabolism. *Arch. Biochem. Biophys.* 94, 449–463.

- Puyol, D., Barry, E.M., Hülsen, T., Batstone, D.J., 2017a. A mechanistic model for anaerobic phototrophs in domestic wastewater applications: Photo-anaerobic model (PANM). *Water Res.* 116, 241–253. <https://doi.org/10.1016/j.watres.2017.03.022>
- Puyol, D., Batstone, D.J., Hülsen, T., Astals, S., Peces, M., Krömer, J.O., 2017b. Resource recovery from wastewater by biological technologies: Opportunities, challenges, and prospects. *Front. Microbiol.* 7, 1–23. <https://doi.org/10.3389/fmicb.2016.02106>
- Rey, F.E., Oda, Y., Harwood, C.S., 2006. Regulation of uptake hydrogenase and effects of hydrogen utilization on gene expression in *Rhodospseudomonas palustris*. *J. Bacteriol.* 188, 6143–6152. <https://doi.org/10.1128/JB.00381-06>
- Ritala, A., Häkkinen, S.T., Toivari, M., Wiebe, M.G., 2017. Single cell protein-state-of-the-art, industrial landscape and patents 2001-2016. *Front. Microbiol.* 8. <https://doi.org/10.3389/fmicb.2017.02009>
- Ruiz-Martínez, A., Serralta, J., Seco, A., Ferrer, J., 2016. Modeling light and temperature influence on ammonium removal by *Scenedesmus* sp. under outdoor conditions. *Water Sci. Technol.* 74, 1964–1970. <https://doi.org/10.2166/wst.2016.383>
- Sasaki, K., Tanaka, T., Nagai, S., 1998. Use of photosynthetic bacteria for the production of SCP and chemicals from organic wastes, in: Martin, A.M. (Ed.), *Bioconversion of Waste Materials to Industrial Products*. Springer US, Boston, MA, pp. 247–292. https://doi.org/10.1007/978-1-4615-5821-7_6
- Schmidt-Rohr, K., 2020. Oxygen Is the High-Energy Molecule Powering Complex Multicellular Life: Fundamental Corrections to Traditional Bioenergetics. *ACS Omega* 5, 2221–2233. <https://doi.org/10.1021/acsomega.9b03352>
- Sepúlveda-Muñoz, C.A., de Godos, I., Puyol, D., Muñoz, R., 2020. A systematic optimization of piggery wastewater treatment with purple phototrophic bacteria. *Chemosphere* 253. <https://doi.org/10.1016/j.chemosphere.2020.126621>

- Sepúlveda-Muñoz, C.A., Hontiyuelo, G., Blanco, S., Torres-Franco, A.F., Muñoz, R., 2022. Photosynthetic treatment of piggery wastewater in sequential purple phototrophic bacteria and microalgae-bacteria photobioreactors. *J. Water Process Eng.* 47. <https://doi.org/10.1016/j.jwpe.2022.102825>
- Sharif, M., Zafar, M.H., Aqib, A.I., Saeed, M., Farag, M.R., Alagawany, M., 2021. Single cell protein: Sources, mechanism of production, nutritional value and its uses in aquaculture nutrition. *Aquaculture* 531, 735885. <https://doi.org/10.1016/j.aquaculture.2020.735885>
- Spanoghe, J., Ost, K.J., Van Beeck, W., Vermeir, P., Lebeer, S., Vlaeminck, S.E., 2022. Purple bacteria screening for photoautohydrogenotrophic food production: Are new H₂-fed isolates faster and nutritionally better than photoheterotrophically obtained reference species? *N. Biotechnol.* 72, 38–47. <https://doi.org/10.1016/j.nbt.2022.08.005>
- Spanoghe, J., Vermeir, P., Vlaeminck, S.E., 2021. Microbial food from light, carbon dioxide and hydrogen gas: Kinetic, stoichiometric and nutritional potential of three purple bacteria. *Bioresour. Technol.* 337, 125364. <https://doi.org/10.1016/j.biortech.2021.125364>
- Tsapekos, P., Khoshnevisan, B., Zhu, X., Zha, X., Angelidaki, I., 2019. Methane oxidising bacteria to upcycle effluent streams from anaerobic digestion of municipal biowaste. *J. Environ. Manage.* 251. <https://doi.org/10.1016/j.jenvman.2019.109590>
- United Nations Department of Economic and Social Affairs, P.D., 2022. World Population Prospects.
- Valverde-Pérez, B., Xing, W., Zachariae, A.A., Skadborg, M.M., Kjeldgaard, A.F., Palomo, A., Smets, B.F., 2020. Cultivation of methanotrophic bacteria in a novel bubble-free membrane bioreactor for microbial protein production. *Bioresour. Technol.* 310, 123388. <https://doi.org/10.1016/j.biortech.2020.123388>
- van Niel, C.B., 1944. the Culture, General Physiology, Morphology, and Classification of the

Non-Sulfur Purple and Brown Bacteria. *Bacteriol. Rev.* 8, 1–118.

<https://doi.org/10.1128/membr.8.1.1-118.1944>

Wágner, D.S., Valverde-Pérez, B., Plósz, B.G., 2018. Light attenuation in photobioreactors and algal pigmentation under different growth conditions – Model identification and complexity assessment. *Algal Res.* 35, 488–499.

<https://doi.org/https://doi.org/10.1016/j.algal.2018.08.019>

Journal Pre-proof

Credit author statement

María del Rosario Rodero: Investigation, Formal analysis, Visualization, Writing-Original draft. **Jose Antonio Magdalena:** Investigation, Writing-Review & Editing. **Jean-Philippe Steyer:** Supervision, Writing-Review & Editing. **Renaud Escudié:** Funding acquisition, Writing-Review & Editing. **Gabriel Capson-Tojo:** Methodology, Formal analysis, Conceptualization, Supervision, Writing-Review & Editing.

Journal Pre-proof

Declaration of interests

The authors declare that they have no known competing financial interests or personal relationships that could have appeared to influence the work reported in this paper.

The authors declare the following financial interests/personal relationships which may be considered as potential competing interests:

Journal Pre-proof

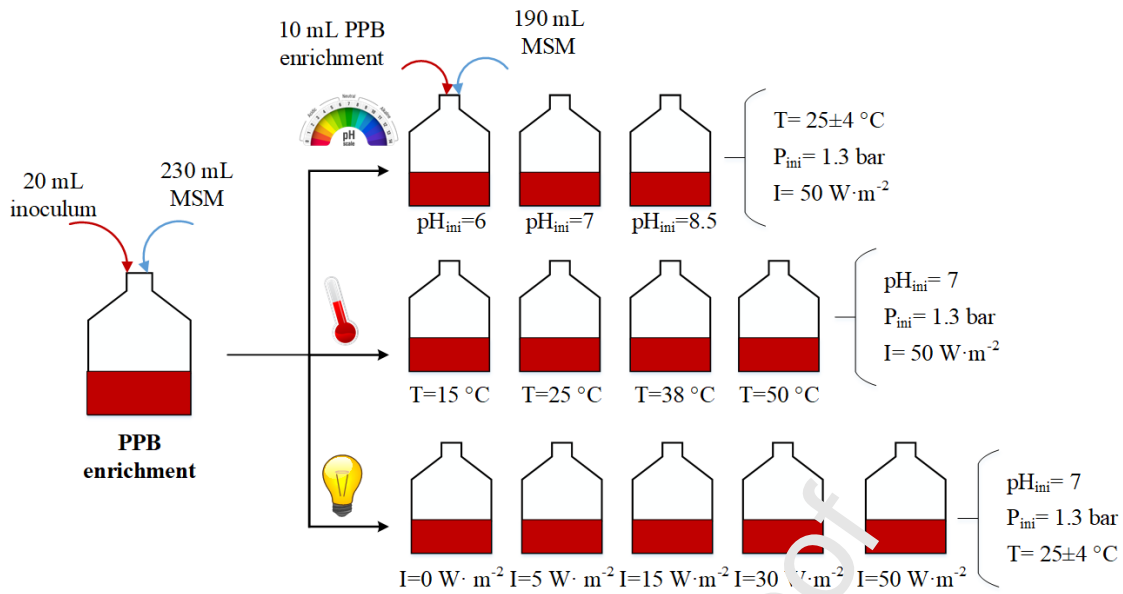


Figure 1. Simplified experimental procedure followed for assessing the influence of environmental conditions (i.e., pH, temperature and light intensity) on the bioconversion of H₂ into SCP using an enriched PPB culture. PPB stands for purple phototrophic bacteria, MSM for mineral medium, T for temperature, P_{ini} for initial pressure and pH_{ini} for initial pH.

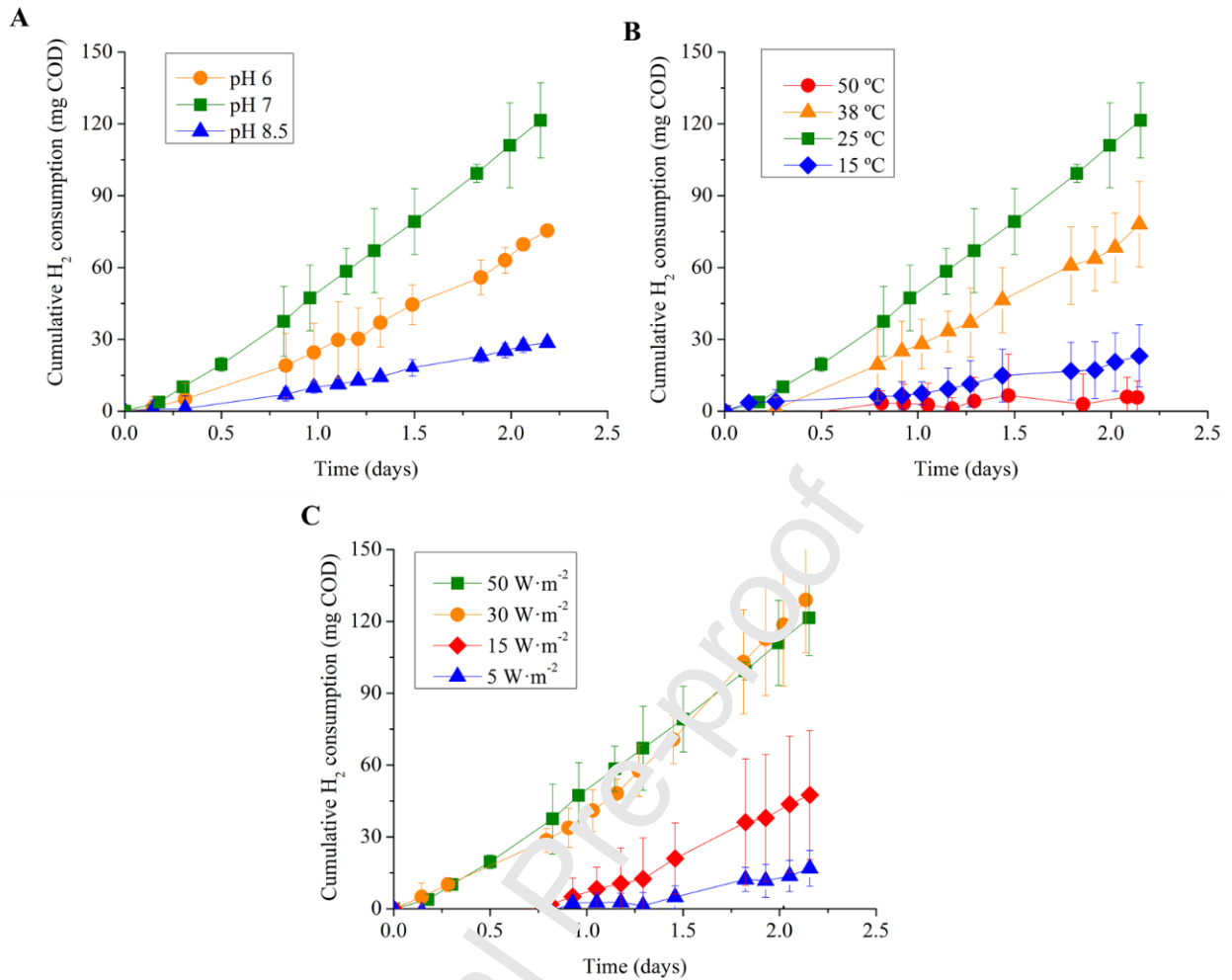


Figure 2. Time course of H₂ consumption (as cumulative H₂ consumed from the headspace) by the enriched PPB cultures at (A) different pH values at 25 °C and light intensity of 50 W·m⁻², (B) different temperatures at initial pH of 7 and light intensity of 50 W·m⁻² and (C) different light intensities at initial pH of 7 and 25 °C. Each data point shows the average and confidence intervals (95%, *n* = 5).

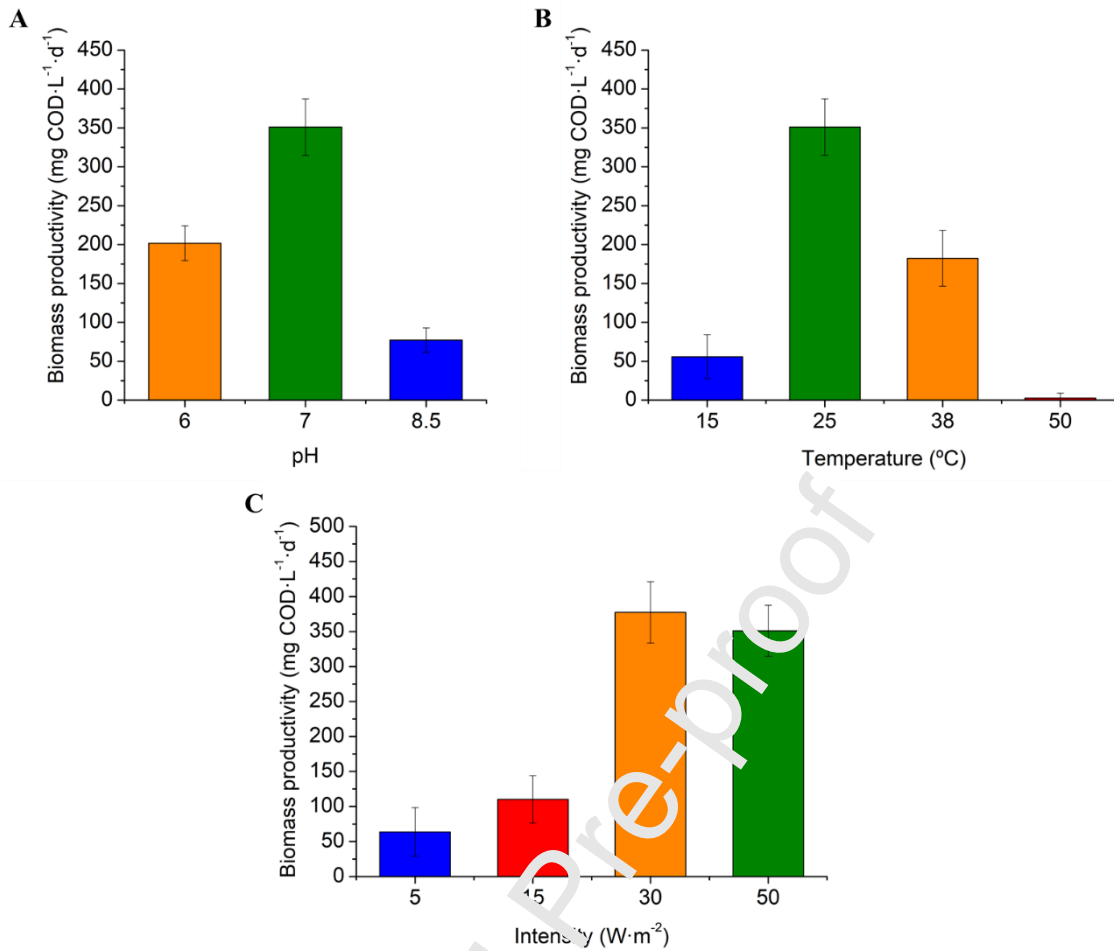


Figure 3. Average biomass productivities at (A) different pH values at 25 °C and light intensity of 50 W·m⁻², (B) different temperatures at initial pH of 7 and light intensity of 50 W·m⁻² and (C) different light intensities at initial pH of 7 and 25 °C. Each bar shows the average and confidence interval (95%, n=12).

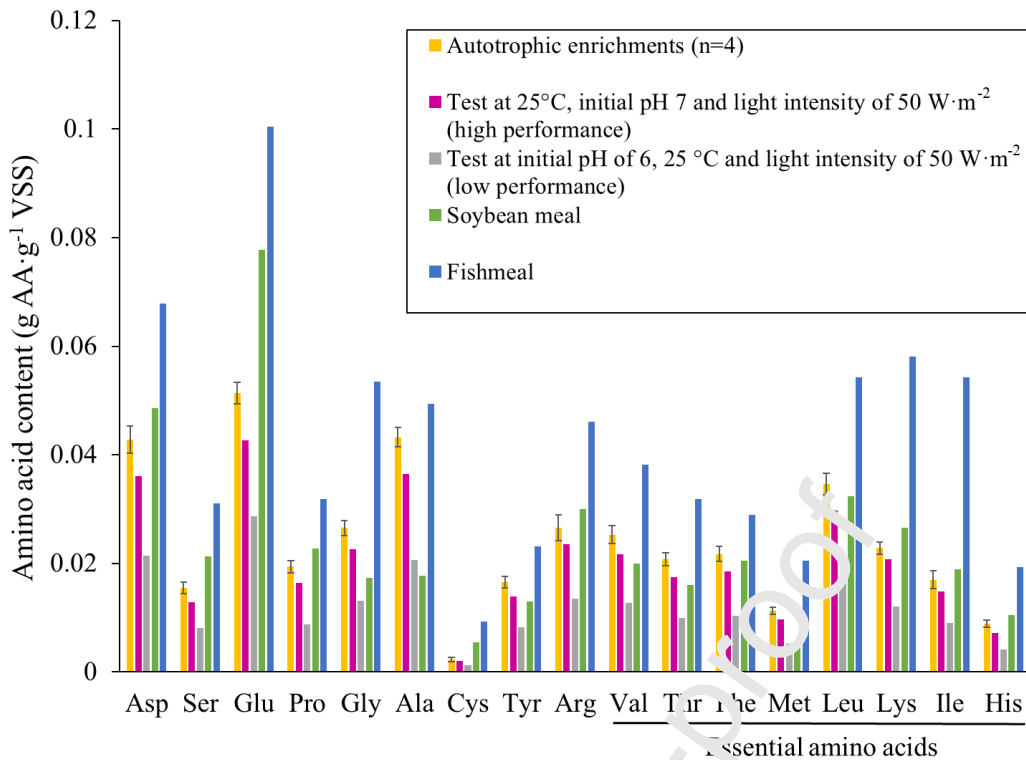


Figure 4. Amino acid (AA) profile of biomass samples at the end of the following tests: autotrophic enrichments (n=4); test at 25°C, initial pH 7 and light intensity of 50 W·m⁻² (high performance); test at initial pH of 6, 25 °C and light intensity of 50 W·m⁻² (low performance). Results are compared to AA profiles of soybean meal and fishmeal (FAO, 1981). AA included are: Aspartic acid+Asparagine (Asp), Serine (Ser), Glutamic acid+Glutamine (Glu), Proline (Pro), Glycine (Gly), Alanine (Ala), Cystine (Cys), Tyrosine (Tyr), Arginine (Arg), Valine (Val), Threonine (Thr), Phenylalanine (Phe), Methionine (Met), Leucine (Leu), Lysine (Lys), Isoleucine (Ile) and Histidine (His).

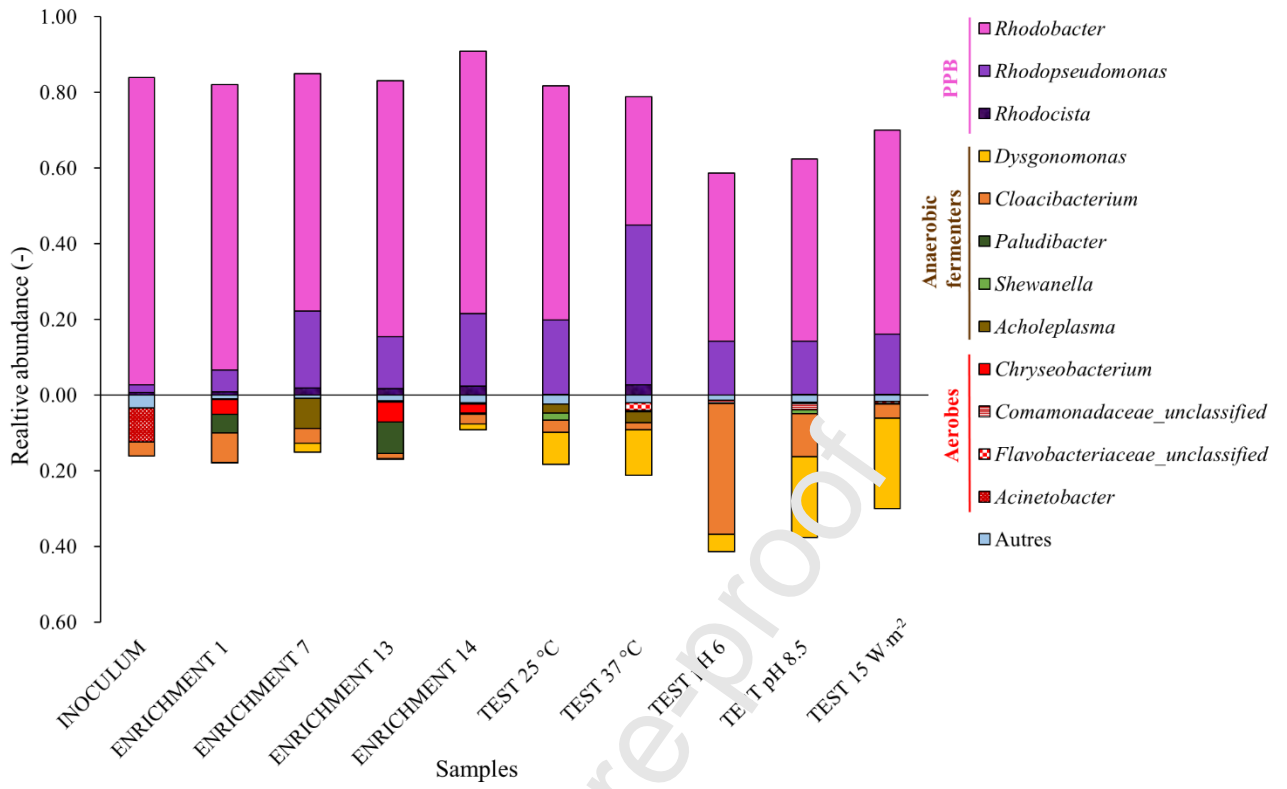


Figure 5. Community structure in the selected samples.

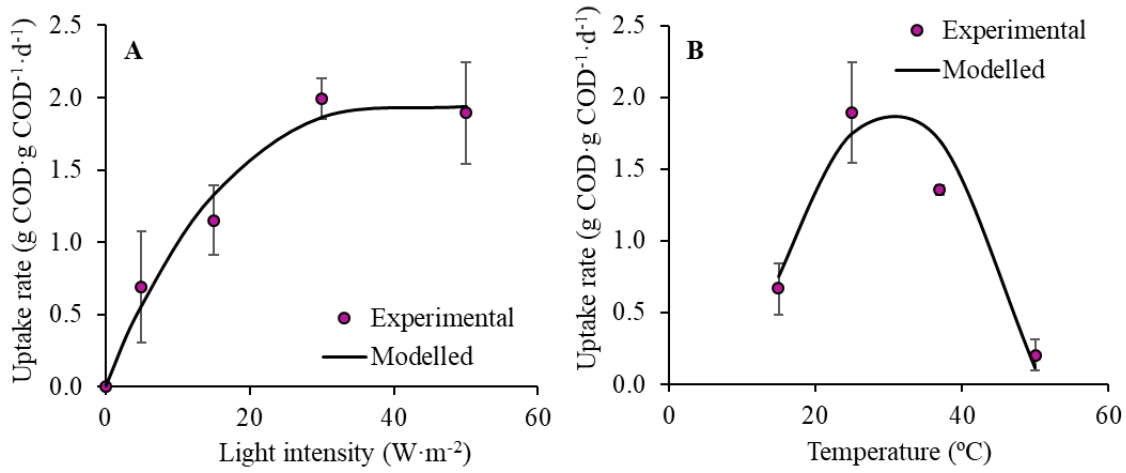


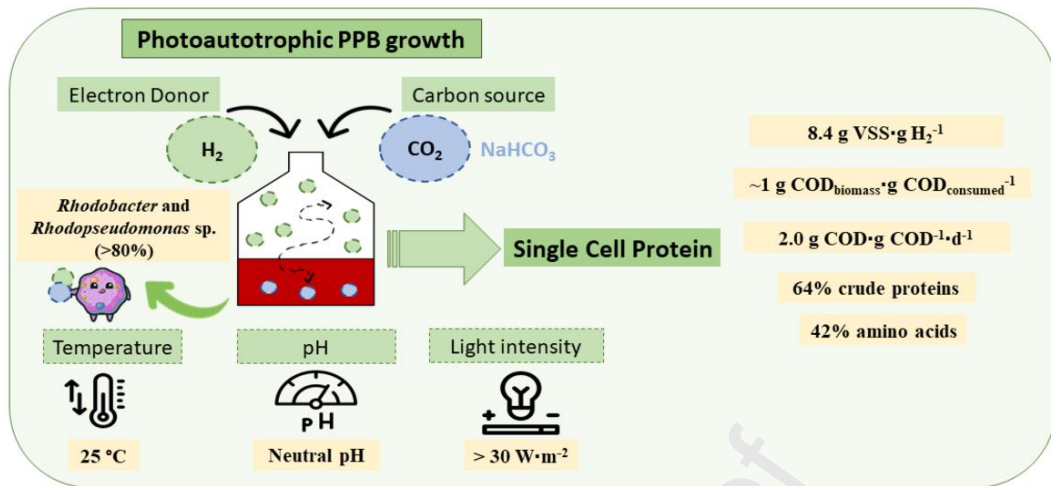
Figure 6. Influence of the (A) light intensity and (B) temperature on the specific H₂ uptake rates. Average and confidence intervals are shown (95% ; n=3). The modelled results correspond to the Steele's equation (light intensity) and the cardinal temperature model with inflection (temperature).

Table 1. Overall and specific H₂ uptake rates, biomass yields and composition, final biomass concentrations, total and soluble Kjeldahl nitrogen (TKN) concentrations, crude protein concentrations and average protein productivities along with the corresponding standard deviations or confidence intervals (95%) during the batch tests (n=3).

	pH			Temperature (°C)				Intensity (W·m ⁻²)			
	6	7	8.5	15	25	38	50	5	15	30	50
Overall H₂ uptake rates (mg COD·d⁻¹)	35±1	58±7	14±1	10±3	58±7	37±3	4±4	9±8	25±6	61±5	58±7
Specific H₂ uptake rates (g COD·g COD⁻¹·d⁻¹)	1.50±0.05	1.89±0.35	0.83±0.02	0.66±0.18	1.89±0.35	1.35±0.04	0.20±0.04	0.69±0.15	1.15±0.24	2.00±0.14	1.89±0.35
Biomass yield (g COD_{biomass}·g COD_{consumed}⁻¹)	1.00±0.17	1.04±0.05	0.93±0.02	0.85±0.18	1.04±0.05	0.99±0.17	0.13±0.02	1.01±0.45	1.02±0.14	1.05±0.05	1.04±0.05
Final biomass concentration (g VSS·L⁻¹)	0.46±0.06	0.79±0.04	0.29±0.02	0.23±0.01	0.79±0.04	0.54±0.02	0.10±0.00	0.19±0.03	0.32±0.02	0.67±0.02	0.79±0.04
Biomass yield (g VSS·g H₂⁻¹)	7.7±0.9	8.2±0.5	6.7±0.4	7.6±0.4	8.2±0.5	8.4±0.3	0.9±0.3	6.6±0.8	6.8±0.19	6.9±0.5	8.2±0.5
TKN_{total} (mg N·L⁻¹)	-*	102±3	101±5	109±2	102±3	107±3	-*	-*	107±0	117±14	102±3
TKN_{soluble} (mg N·L⁻¹)	-*	37±7	74±3	87±3	37±7	63±4	-*	-*	70±8	41±3	37±7
Crude protein content (%)	-*	51±5	59±7	54±5	51±5	50±6	-*	-*	61±4	64±1	51±5
Average protein productivities (g protein·L⁻¹·d⁻¹)	-*	0.18±0.02	0.04±0.01	0.04±0.02	0.18±0.02	0.10±0.02	-*	-*	0.03±0.02	0.20±0.03	0.18±0.02
C content of biomass (%w·w⁻¹)	42±1	41±2	-*	41±1	41±2	41±1	-*	-*	44±0	43±3	41±2
N content of biomass (%w·w⁻¹)	8±1	10±0	-*	8±0	10±0	9±0	-*	-*	10±0	10±1	10±0
H content of biomass (%w·w⁻¹)	6±0	6±0	-*	6±0	6±0	6±0	-*	-*	6±0	6±0	6±0

* These results could not be determined due to the low final biomass concentrations in these tests.

Graphical abstract



Highlights

- The bioconversion of H₂ into SCP by an enriched PPB consortium was studied
- High biomass yields were reached (up to 1 g COD_{biomass}·g COD_{consumed}⁻¹)
- PPB biomass had high protein contents (>50%) and adequate amino acid profiles
- Neutral pH, 25°C and light intensities >30 W·m⁻² were optimal for PPB growth
- A mechanistic model to represent biomass growth and H₂ uptake was proposed

Journal Pre-proof